

GEOARCHAEOLOGICAL XRF LAB

ARCHAEOLOGICAL X-RAY FLUORESCENCE SPECTROMETRY LABORATORY
8100 WYOMING BLVD., SUITE M4-158

ALBUQUERQUE, NM 87113 USA

**SOURCE PROVENANCE OF A BIPOLAR OBSIDIAN ARTIFACT ASSEMBLAGE FROM
FIVE SITES IN SOUTHERN NEW MEXICO**

by

M. Steven Shackley Ph.D., Director
Geoarchaeological XRF Laboratory
Albuquerque, New Mexico

Report Prepared for

Adam Okun
Parametrix
Albuquerque, New Mexico

25 May 2013

INTRODUCTION

The analysis here of 27 obsidian artifacts from five sites in southern New Mexico indicates procurement most likely from nearby Rio Grande Quaternary alluvium (Church 2000; Shackley 2012; Tables 1 and 2). The dominant source is Cerro Toledo Rhyolite, the most common secondarily deposited obsidian in the Rio Grande alluvium, the primary sources of which are at Valles Caldera, Jemez Mountains, followed by the two Mount Taylor sources that have eroded into the Rio Puerco and into the Rio Grande, and the Tertiary Period pre-caldera Canovas Canyon Rhyolite (Bear Springs Peak) source that has been found as far south as the Las Cruces area (Church 2000). The mix of sources by site is probably not significant, based on an encounter strategy in procurement (see Tables 1 and 2).

LABORATORY SAMPLING, ANALYSIS AND INSTRUMENTATION

All archaeological samples are analyzed whole. The results presented here are quantitative in that they are derived from "filtered" intensity values ratioed to the appropriate x-ray continuum regions through a least squares fitting formula rather than plotting the proportions of the net intensities in a ternary system (McCarthy and Schamber 1981; Schamber 1977). Or more essentially, these data through the analysis of international rock standards, allow for inter-instrument comparison with a predictable degree of certainty (Hampel 1984; Shackley 2011).

All analyses for this study were conducted on a ThermoScientific *Quant'X* EDXRF spectrometer, located in the Archaeological XRF Laboratory, Albuquerque, New Mexico. It is equipped with a thermoelectrically Peltier cooled solid-state Si(Li) X-ray detector, with a 50 kV, 50 W, ultra-high-flux end window bremsstrahlung, Rh target X-ray tube and a 76 μm (3 mil) beryllium (Be) window (air cooled), that runs on a power supply operating 4-50 kV/0.02-1.0 mA at 0.02 increments. The spectrometer is equipped with a 200 l min^{-1} Edwards vacuum pump, allowing for the analysis of lower-atomic-weight elements between sodium (Na) and titanium

(Ti). Data acquisition is accomplished with a pulse processor and an analogue-to-digital converter. Elemental composition is identified with digital filter background removal, least squares empirical peak deconvolution, gross peak intensities and net peak intensities above background.

The analysis for mid Zb condition elements Ti-Nb, Pb, Th, the x-ray tube is operated at 30 kV, using a 0.05 mm (medium) Pd primary beam filter in an air path at 200 seconds livetime to generate x-ray intensity Ka-line data for elements titanium (Ti), manganese (Mn), iron (as Fe_2O_3^T), cobalt (Co), nickel (Ni), copper, (Cu), zinc, (Zn), gallium (Ga), rubidium (Rb), strontium (Sr), yttrium (Y), zirconium (Zr), niobium (Nb), lead (Pb), and thorium (Th). Not all these elements are reported since their values in many volcanic rocks are very low. Trace element intensities were converted to concentration estimates by employing a least-squares calibration line ratioed to the Compton scatter established for each element from the analysis of international rock standards certified by the National Institute of Standards and Technology (NIST), the US. Geological Survey (USGS), Canadian Centre for Mineral and Energy Technology, and the Centre de Recherches Pétrographiques et Géochimiques in France (Govindaraju 1994). Line fitting is linear (XML) for all elements but Fe where a derivative fitting is used to improve the fit for iron and thus for all the other elements. When barium (Ba) is analyzed in the High Zb condition, the Rh tube is operated at 50 kV and up to 1.0 mA, ratioed to the bremsstrahlung region (see Davis 2011; Shackley 2011). Further details concerning the petrological choice of these elements in Southwest obsidians is available in Shackley (1988, 1995, 2005; also Mahood and Stimac 1991; and Hughes and Smith 1993). Nineteen specific pressed powder standards are used for the best fit regression calibration for elements Ti-Nb, Pb, Th, and Ba, include G-2 (basalt), AGV-2 (andesite), GSP-2 (granodiorite), SY-2 (syenite), BHVO-2 (hawaiiite), STM-1 (syenite), QLO-1 (quartz latite), RGM-1 (obsidian), W-2 (diabase),

BIR-1 (basalt), SDC-1 (mica schist), TLM-1 (tonalite), SCO-1 (shale), NOD-A-1 and NOD-P-1 (manganese) all US Geological Survey standards, NIST-278 (obsidian), U.S. National Institute of Standards and Technology, BE-N (basalt) from the Centre de Recherches Pétrographiques et Géochimiques in France, and JR-1 and JR-2 (obsidian) from the Geological Survey of Japan (Govindaraju 1994).

The data from the WinTrace software were translated directly into Excel for Windows software for manipulation and on into SPSS for Windows for statistical analyses. In order to evaluate these quantitative determinations, machine data were compared to measurements of known standards during each run. RGM-1 a USGS obsidian standard is analyzed during each sample run for obsidian artifacts to check machine calibration (Table 1). Source assignments were made by reference to Shackley (1995, 2005) and source standard data at this lab (Table 1, Figures 1 and 2).

REFERENCES CITED

- Davis, K.D., T.L. Jackson, M.S. Shackley, T. Teague, and J.H. Hampel
2011 Factors Affecting the Energy-Dispersive X-Ray Fluorescence (EDXRF) Analysis of Archaeological Obsidian. In *X-Ray Fluorescence Spectrometry (XRF) in Geoarchaeology*, edited by M.S. Shackley, pp. 45-64. Springer, New York.
- Govindaraju, K.
1994 1994 Compilation of Working Values and Sample Description for 383 Geostandards. *Geostandards Newsletter* 18 (special issue).
- Hampel, Joachim H.
1984 Technical Considerations in X-ray Fluorescence Analysis of Obsidian. In *Obsidian Studies in the Great Basin*, edited by R.E. Hughes, pp. 21-25. Contributions of the University of California Archaeological Research Facility 45. Berkeley.
- Hildreth, W.
1981 Gradients in Silicic Magma Chambers: Implications for Lithospheric Magmatism. *Journal of Geophysical Research* 86:10153-10192.
- Hughes, Richard E., and Robert L. Smith
1993 Archaeology, Geology, and Geochemistry in Obsidian Provenance Studies. In *Scale on Archaeological and Geoscientific Perspectives*, edited by J.K. Stein and A.R. Linse, pp. 79-91. Geological Society of America Special Paper 283.

Mahood, Gail A., and James A. Stimac

1990 Trace-Element Partitioning in Pantellerites and Trachytes. *Geochemica et Cosmochimica Acta* 54:2257- 2276.

McCarthy, J.J., and F.H. Schamber

1981 Least-Squares Fit with Digital Filter: A Status Report. In *Energy Dispersive X-ray Spectrometry*, edited by K.F.J. Heinrich, D.E. Newbury, R.L. Myklebust, and C.E. Fiori, pp. 273-296. National Bureau of Standards Special Publication 604, Washington, D.C.

Schamber, F.H.

1977 A Modification of the Linear Least-Squares Fitting Method which Provides Continuum Suppression. In *X-ray Fluorescence Analysis of Environmental Samples*, edited by T.G. Dzubay, pp. 241-257. Ann Arbor Science Publishers.

Shackley, M. Steven

1988 Sources of Archaeological Obsidian in the Southwest: An Archaeological, Petrological, and Geochemical Study. *American Antiquity* 53(4):752-772.

1995 Sources of Archaeological Obsidian in the Greater American Southwest: An Update and Quantitative Analysis. *American Antiquity* 60(3):531-551.

2005 *Obsidian: Geology and Archaeology in the North American Southwest*. University of Arizona Press, Tucson.

2011 An Introduction to X-Ray Fluorescence (XRF) Analysis in Archaeology. In *X-Ray Fluorescence Spectrometry (XRF) in Geoarchaeology*, edited by M.S. Shackley, pp. 7-44. Springer, New York.

2012 The Secondary Distribution of Archaeological Obsidian in Rio Grande Quaternary Sediments, Jemez Mountains to San Antonito, New Mexico: Inferences for Prehistoric Procurement and the Age of Sediments. Poster presentation at the Society for American Archaeology, Annual Meeting, Memphis, Tennessee.

Table 1. Elemental concentrations and source assignments for the archaeological specimens, and analysis of USGS RGM-1 obsidian standard. All measurements in parts per million (ppm).

Site	Sample	Ti	Mn	Fe	Zn	Rb	Sr	Y	Zr	Nb	Pb	Th	Source
LA	23.1	537	46	1180	99	20	8	64	17	92	36	16	Cerro Toledo Rhy
169064			9	1		2			1				
LA	219.1	291	18	8434	14	-1	10	1	9	4	0	9	not obsidian
169064			2										
LA	242.1	640	48	1213	14	20	8	64	17	97	35	25	Cerro Toledo Rhy
169064			8	8	5	8			5				
LA	243.1	768	37	1048	46	11	42	24	99	51	24	25	Canovas Canyon Rhy
169064			7	0		7							
LA	341.1	524	48	1177	11	19	10	63	16	95	34	27	Cerro Toledo Rhy
169064			1	4	9	6			5				
LA	414.1	602	48	1209	11	20	9	64	17	10	37	34	Cerro Toledo Rhy
169064			9	0	5	6			7	0			
LA	488.1	729	48	1204	12	19	9	62	16	98	34	22	Cerro Toledo Rhy
169064			0	7	7	8			4				
LA	546.1	538	46	1163	10	20	8	63	16	93	35	28	Cerro Toledo Rhy
169064			0	9	0	0			5				
LA	563.1	540	45	1164	92	19	8	61	16	97	32	23	Cerro Toledo Rhy
169064			1	0		8			9				
LA	587.1	589	47	1203	92	20	9	64	17	94	34	24	Cerro Toledo Rhy
169064			8	7		5			3				
LA	601.1	679	50	1216	10	20	11	63	16	94	37	25	Cerro Toledo Rhy
169064			3	7	4	5			8				
LA	630	590	45	1170	10	19	9	63	16	89	38	17	Cerro Toledo Rhy
169064			6	5	4	4			8				
LA	659.1	565	52	1178	18	48	13	86	13	22	54	29	Mt Taylor/Horace Mesa
169064			8	4	8	7			1	7			
LA	663.1	595	54	1259	15	23	9	64	17	10	41	31	Cerro Toledo Rhy
169064			6	9	4	2			8	2			
LA	668.1	798	69	1309	36	58	13	86	13	21	68	20	Mt. Taylor/Horace Mesa
169064			6	7	4	1			6	7			
LA	4.1	756	53	1267	12	21	8	64	17	10	38	32	Cerro Toledo Rhy
169066			9	3	3	0			2	0			
LA	21.1	961	47	1221	16	19	8	59	16	94	37	22	Cerro Toledo Rhy
169066			2	3	2	8			3				
LA	69.1	416	68	1093	17	54	10	80	11	19	62	27	Mt Taylor/Grants Ridge
169066			5	3	2	5			4	6			
LA	79.1	853	56	1327	25	22	8	64	17	96	43	28	Cerro Toledo Rhy
169066			7	0	9	4			2				
LA	12.1	678	48	1228	10	20	8	61	17	98	37	20	Cerro Toledo Rhy
169077			3	1	7	8			4				
LA	27.1-1	622	41	1143	99	18	9	59	16	90	32	23	Cerro Toledo Rhy
169077			6	2		2			1				
LA	27.1-2	689	49	1235	12	21	10	60	18	99	37	27	Cerro Toledo Rhy
169077			2	7	1	6			0				
LA	28.1	640	48	1226	10	20	10	61	17	10	35	23	Cerro Toledo Rhy
169077			7	1	8	9			8	2			
LA	36.1	830	49	1285	11	21	8	62	17	10	37	27	Cerro Toledo Rhy
169077			8	5	8	3			9	2			
LA	47.1	780	48	1212	11	19	12	62	16	92	34	21	Cerro Toledo Rhy
169077			0	3	6	4			2				
LA	6	718	55	1285	19	22	8	63	17	10	38	24	Cerro Toledo Rhy

169075			6	3	0	5			7	0			
LA	182	642	49	1225	11	22	8	65	17	95	37	22	Cerro Toledo Rhy
169065			7	0	8	0			2				
standard	RGM1-S4	160	28	1374	37	14	10	23	21	7	23	20	standard
		0	9	4		9	9		5				
standard	RGM1-S4	151	28	1379	36	15	10	25	22	8	22	16	standard
		1	0	6		4	6		2				

Table 2. Site by source crosstabulation.

Site * Source Crosstabulation

			Source					Total
			Canovas Canyon Rhy	Cerro Toledo Rhy	Mt Taylor/Grants Ridge	Mt Taylor/Horace Mesa	not obsidian	
Site	LA 169064	Count	1	11	0	2	1	15
		% within Site	6.7%	73.3%	.0%	13.3%	6.7%	100.0%
		% within Source	100.0%	50.0%	.0%	100.0%	100.0%	55.6%
		% of Total	3.7%	40.7%	.0%	7.4%	3.7%	55.6%
	LA 169065	Count	0	1	0	0	0	1
		% within Site	.0%	100.0%	.0%	.0%	.0%	100.0%
		% within Source	.0%	4.5%	.0%	.0%	.0%	3.7%
		% of Total	.0%	3.7%	.0%	.0%	.0%	3.7%
	LA 169066	Count	0	3	1	0	0	4
		% within Site	.0%	75.0%	25.0%	.0%	.0%	100.0%
		% within Source	.0%	13.6%	100.0%	.0%	.0%	14.8%
		% of Total	.0%	11.1%	3.7%	.0%	.0%	14.8%
	LA 169075	Count	0	1	0	0	0	1
		% within Site	.0%	100.0%	.0%	.0%	.0%	100.0%
		% within Source	.0%	4.5%	.0%	.0%	.0%	3.7%
		% of Total	.0%	3.7%	.0%	.0%	.0%	3.7%
LA 169077	Count	0	6	0	0	0	6	
	% within Site	.0%	100.0%	.0%	.0%	.0%	100.0%	
	% within Source	.0%	27.3%	.0%	.0%	.0%	22.2%	
	% of Total	.0%	22.2%	.0%	.0%	.0%	22.2%	
Total	Count	1	22	1	2	1	27	
	% within Site	3.7%	81.5%	3.7%	7.4%	3.7%	100.0%	
	% within Source	100.0%	100.0%	100.0%	100.0%	100.0%	100.0%	
	% of Total	3.7%	81.5%	3.7%	7.4%	3.7%	100.0%	

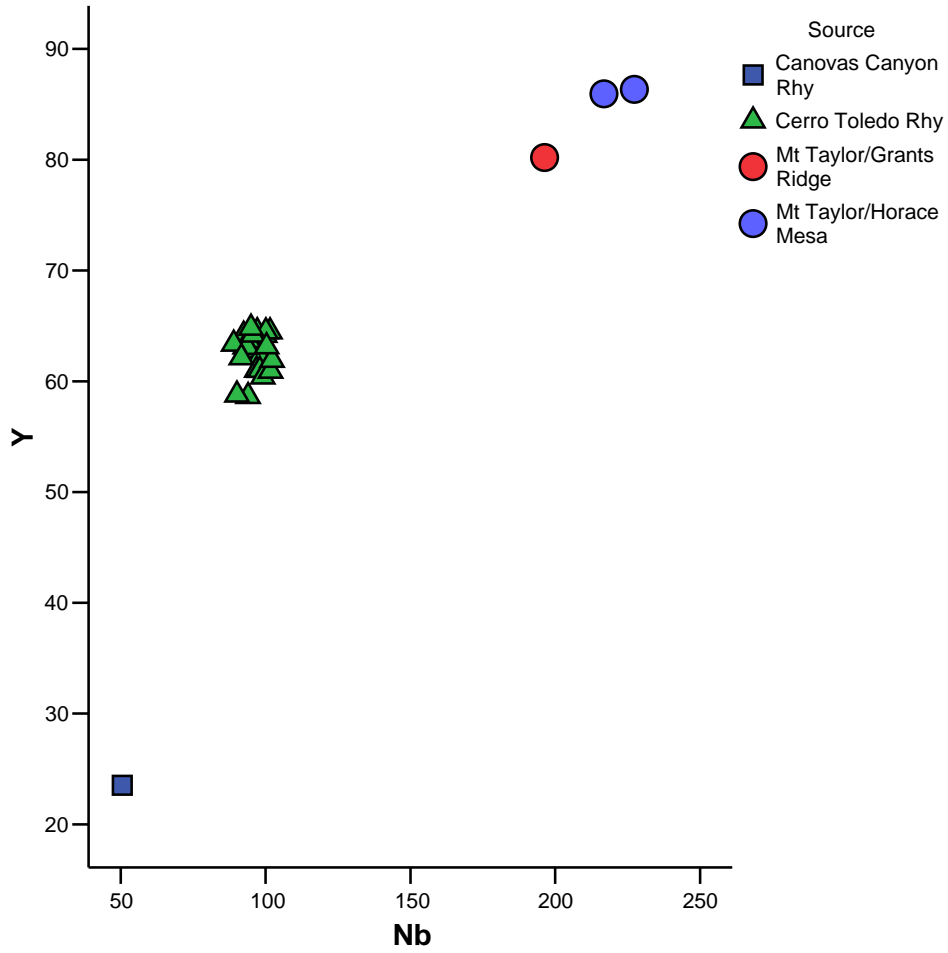


Figure 1. Y versus Nb bivariate plot of the archaeological specimens.

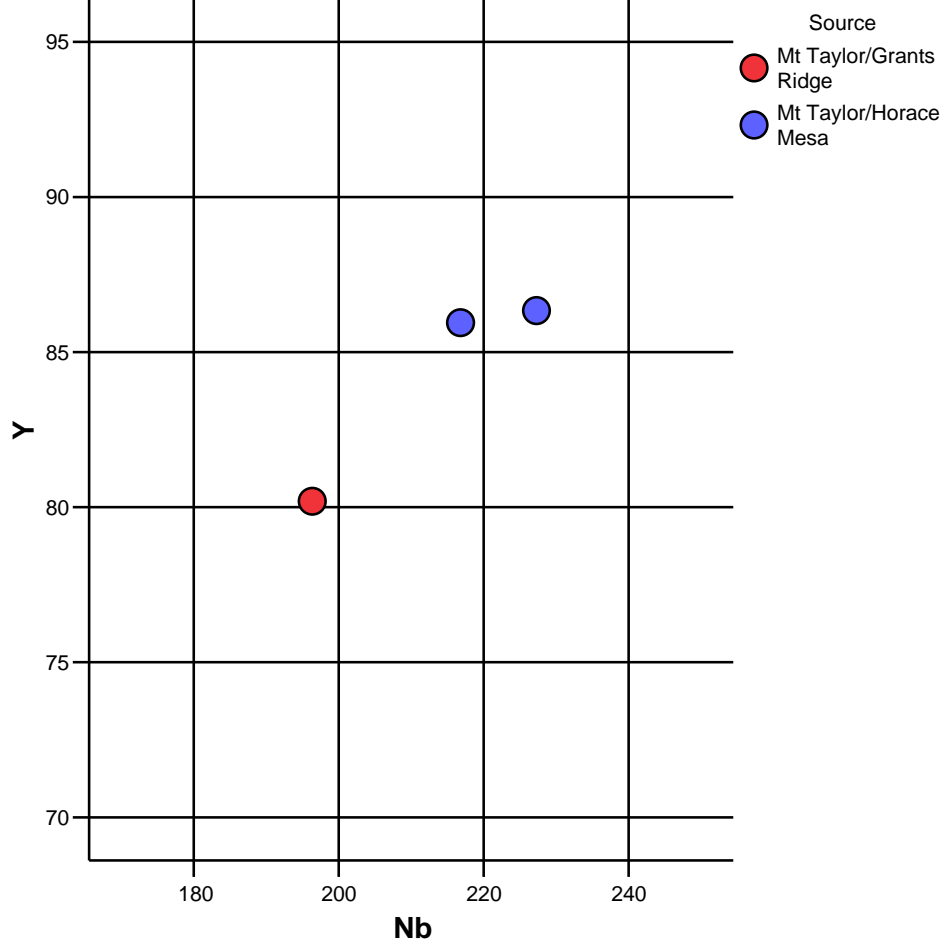


Figure 1. Y versus Nb bivariate plot of the Mount Taylor source locality assignments providing better discrimination (see Shackley 2005: 58-64).